

Immune landscape of the affected brain in Rasmussen encephalitis

Received: 12 January 2026

Accepted: 27 April 2026

Published online: 13 May 2026

Cite this article as: Quinones-Valdez G., Chang J.W., Magaki S.D. *et al.* Immune landscape of the affected brain in Rasmussen encephalitis. *Sci Rep* (2026). <https://doi.org/10.1038/s41598-026-51295-3>

Giovanni Quinones-Valdez, Julia W. Chang, Shino D. Magaki, Harry V. Vinters, Noriko Salamon, Anthony C. Wang, Aria Fallah & Geoffrey C. Owens

We are providing an unedited version of this manuscript to give early access to its findings. Before final publication, the manuscript will undergo further editing. Please note there may be errors present which affect the content, and all legal disclaimers apply.

If this paper is publishing under a Transparent Peer Review model then Peer Review reports will publish with the final article.

ARTICLE IN PRESS

Immune landscape of the affected brain in Rasmussen encephalitis

Giovanni Quinones-Valdez¹, Julia W. Chang², Shino D. Magaki², Harry V. Vinters^{2,3}, Noriko Salamon⁴, Anthony C. Wang⁵, Aria Fallah⁵, and Geoffrey C. Owens^{5*}

Department of Integrative Biology and Physiology¹, College of Life Sciences, University of California Los Angeles, Division of Neuropathology, Department of Pathology and Laboratory Medicine², Departments of Neurology³, Radiological Sciences⁴ and Neurosurgery⁵, David Geffen School of Medicine, University of California Los Angeles, Los Angeles, CA, USA.

*Corresponding author: Department of Neurosurgery, David Geffen School of Medicine at UCLA, 300 Stein Plaza, Ste. 562, Los Angeles, CA 90095-6901

Email: geoffreyowens@mednet.ucla.edu

Abstract

Rasmussen encephalitis (RE) is a rare neuroinflammatory disease characterized by intractable seizures and progressive brain atrophy that is usually confined to one cerebral hemisphere. Disease management involves anti-seizure medications and immunotherapy, although surgical resection remains the only effective treatment option to achieve seizure freedom. The presence of clonally expanded resident memory T cells in brain tissue removed to control seizures suggests the involvement of an autoimmune response in the etiology of the disease. Blocks of fresh brain tissue were obtained from three RE surgery cases (ages 5, 8, and 26 years at the time of surgery) and immune cells were isolated. Single cell RNA sequencing was used to define the types of immune cells present in the affected brain tissue and potential crosstalk between them, along with multiplex immunofluorescence immunostaining of sections from the same specimens. We matched T cell receptor sequences to T cell phenotypes and used ViralTrack software to search for evidence of activation of latent viruses in the immune cells. The immune cells isolated from the three RE cases comprised primarily activated microglia and resident memory CD8 T cells with fewer CD4 T cells, NK cells and monocyte-derived macrophages and dendritic cells. The majority of CD8 T cells expressed killer cell lectin-like receptors, and a virus responsive gene signature that included XCL1, TNFRSF9 and CRTAM, but also the exhaustion markers LAG-3 and TIM-3. Microglia expressed transcripts found in disease-associated microglia and transcripts associated with NLRP3 inflammasomes. We found no evidence for active latent viruses; however, we found endogenous HERV-K retrovirus sequences that were transcribed from multiple provirus insertion sites.

Key words: Rasmussen encephalitis, T cells, microglia, single cell RNA sequencing, endogenous retrovirus

Background

Rasmussen encephalitis (RE) is a rare neuroinflammatory disease characterized by seizures and progressive brain atrophy that is usually confined to one cerebral hemisphere [14, 84, 122], although bilateral cases have been described [92]. In a recent retrospective study of 160 RE cases, the median age of clinical onset was seven years (range 1 to 53 years) with the left cerebral hemisphere more often affected [39]. Disease management involves immunotherapy and anti-seizure medications (ASMs) although surgical resection remains the only effective treatment option to achieve seizure freedom [50, 85]. The presence of clonally focused T cells in resected involved brain tissue suggests that RE may have an autoimmune component [2, 28, 103, 104], however, to date no T cell specific self-antigens have been identified. Comorbidity with several autoimmune diseases has indicated a potential heritable predisposition [4], and, in support of this idea, we identified HLA class I and II alleles in a cohort of 24 RE surgical cases that have been linked to susceptibility to autoimmune diseases [28]. HLA class II nonsynonymous single nucleotide polymorphisms (SNP) were also found to be enriched in RE cases as well as several SNPs in other genes including those involved in an immune response [1, 68]. Takahashi et al. [113] identified SNPs in *CTLA4* and *PDCD1* that were overrepresented in a cohort of Japanese RE patients, which may negatively affect the function of these immune regulatory genes. Wang et al. identified a SNP in *IFITM3* in Chinese RE patients that may promote human cytomegalovirus (HHV5) persistence in the brain [130]. Epstein Barr virus (HHV4) has been proposed as a viral trigger for Multiple sclerosis (MS) [16], and HHV4, HHV5, and HHV6 sequences have been reported in some RE brain specimens but not in others [8, 38, 69, 78, 94, 127]. In support of a possible viral etiology, early treatment of two presumptive RE cases with ganciclovir was reported to stop seizures and resolve neurological deficits [77, 78]. We found that many of the expanded T

cell clonotypes in RE brain specimens were public suggesting that they may have been directed against a common infectious agent [28]. On the other hand, autoreactive T cell clonotypes may be present in healthy individuals [37].

Co-existence of RE and focal cortical dysplasia (FCD) pathologies has also been documented in RE surgical cases suggesting that FCD could be involved in triggering the disease [43, 51, 114]. FCD is caused by somatic mutations in neural progenitors that occur during early brain development resulting in focal seizures [12]. It has been established that seizures can promote brain inflammation [67, 124], suggesting that seizure activity per se could trigger an inflammatory cascade leading to an autoimmune response.

From the recent large cohort retrospective study of RE cases [39], it was found that the number of RE patients with twin siblings was higher compared with the general population, leading the authors to suggest that the risks of complications associated with preterm births, which are more prevalent in twin pregnancies [118], may also be causative. For example, preterm birth is a risk factor for perinatal arterial ischemic stroke, which may in turn be linked to neuroinflammation and seizures [46, 97].

RNA sequencing of nuclei isolated from resected brain tissue confirmed earlier findings [95, 135] and revealed the heterogeneity of activated microglia in affected brain areas [133]. Based on the pathological stages of RE described by Pardo et al. [89], activation of microglia was shown to occur prior to T cell infiltration [119]. In the present study we have sequenced RNA from individual immune cells isolated from three RE surgery cases and characterized the transcriptomes of both myeloid and lymphocyte populations including T cell receptors. We also present evidence for the reactivation of the endogenous retrovirus HERV-K in these cells.

Methods and Materials

This study was approved by the UCLA Institutional Review Board (IRB no. 18-001048). The patients or their parents or legal guardians provided informed consent for the use of the surgical remnant and blood for research purposes according to the Declaration of Helsinki. There were no exclusion criteria, and no reported comorbidities. All specimens were collected using the same standard operating procedures. De-identified patient information including age at seizure onset, age at surgery, and gender was collected with informed consent.

Single cell RNA sequencing

Immune cells were isolated from blocks of fresh resected brain tissue as previously described [87]. In brief, brain tissue collected from the operating room in ice cold Hibernate® containing penicillin/streptomycin (120U/ml and 100ug/ml respectively, ThermoFisher, Carlsbad, CA) was transferred to magnesium calcium free Hanks Balanced Salt Solution containing HEPES (20mM), glucose (5mM) and penicillin/streptomycin (ThermoFisher), and finely minced on ice with spring scissors. Tissue fragments were transferred to RPMI (ThermoFisher) containing 10% human serum (Phoenix Scientific, San Marcos, CA) and HEPES (20mM) and digested overnight at room temperature with Type IV collagenase (~800U/ml) (Worthington Biochemical Corp. Lakewood, NJ) followed by fractionation on a 70%:30% Percoll® (Millipore Sigma, St. Louis MO) step gradient. The immune cells were collected from the interface between the two Percoll® steps, and two Chromium single cell gene expression libraries (5' gene expression and TCR V(D)J) were prepared (10X Genomics, Pleasanton, CA) and sequenced on a NovaSeq 6000 instrument in a SP flow cell (2x50 bp) (Illumina Inc., San Diego, CA). Reads were demultiplexed and aligned to the Genome Reference Consortium Human Reference 38 (GRCh Build 38) and VDJ reference data (based on Ensembl 94 release) using Cell Ranger count and Cell Ranger VDJ pipelines (10X

Genomics). The single cell RNA sequencing (scRNA-seq) data from the 5' expression library were analyzed using the R package SingCellaR with the default settings [129]. The scRNA-seq data from each RE sample were combined using the integration function from Seurat [48]. Clusters of putative T cells and NK cells (n =10,971) were then extracted, reintegrated using Harmony [66], and re-clustered. Clusters of putative myeloid cells (n= 12,877) were also extracted, reintegrated and re-clustered. The R package Monocle 3.0 [23] was used to perform a trajectory analysis of the myeloid cells. The all_contig_annotations file from the Cell Ranger VDJ pipeline was used to assess the clonotype diversity in each RE sample, and to assign T cell phenotypes to the clonotypes based on the SingCellaR workflow. Spectratyping was performed with the immunarch R package [115], and diversity estimates were calculated using the iNEXT R package [54]. Chord diagrams were made with the R package chorddiag [40]. Barcodes of the most abundant clonotype(s) in each sample were integrated into the SingCellaR object for visualization in UMAP projections. The Metascape web portal was used for pathway analysis [141].

Bioinformatics analysis of cell-cell communication

Myeloid cell and T cell/NK cell SingCellaR objects were converted to Scanpy (v1.11.5)-compatible .h5ad format. Datasets were subsequently merged, and raw counts were re-normalized using \log_2 counts per million (logCPM). Cell–cell communication (CCC) analysis was performed using LIANA+ (v1.7.1) [32]. Multiple methods implemented within LIANA were applied, requiring that at least 20% of cells express the ligand or receptor gene and a minimum of 440 cells per interacting group (corresponding to 20% of the smallest cluster, monocytes-derived cells). The consensus ligand–receptor resource provided by LIANA was used, which integrates expert-curated databases including CellPhoneDB, CellChat, ICELLNET, connectomeDB2020, and CellTalkDB. LIANA's built-in rank aggregation framework was applied alongside multiple individual CCC

inference methods, including CellChat [59], CellPhoneDB [35], Connectome [96], NATMI [53] and SingleCellSignalR [22] as well as summary metrics such as geometric mean and \log_2 fold change (\log_2FC) [33]. Interactions within the same cell type were excluded from downstream analyses. Method-specific filtering criteria were applied to identify high-confidence ligand–receptor pairs. For methods providing statistical significance (CellPhoneDB, geometric mean, and CellChat), p-values were adjusted using the Benjamini–Hochberg procedure, and interactions with adjusted p-values < 0.05 were retained. These interactions were ranked using method-specific magnitude metrics, including *lr_probs* (CellChat), *lr_means* (CellPhoneDB), and *lr_gmeans* (geometric mean). For other methods, the following thresholds were applied: $\log_2FC > 0.5$; Connectome ligand or receptor z-score > 0 ; NATMI specificity weight > 0.1 ; and SingleCellSignalR *lrscore* > 0.5 . For each method, interactions passing these thresholds were ranked according to their respective scoring metrics. The rank aggregation framework (*RankAggregate*) implemented in LIANA+, and based on the Robust Rank Aggregation (RRA) algorithm [65], was used to derive the consensus specificity and magnitude rankings. This approach assigns a probabilistic score to each ligand–receptor pair based on its relative ranking across multiple methods, thereby prioritizing interactions that are consistently highly ranked. Finally, ligand–receptor pairs with a specificity rank ≤ 0.2 were retained, consistent with previous studies [7].

Identification of Viral RNA using ViralTrack

For each sample, processing of the raw RNA sequencing reads was carried out using Umitools [109]. Initially, a whitelist of acceptable barcodes was generated, allowing for a Hamming distance of 1. Subsequently, the barcode sequences were extracted from the reads and incorporated into the read names. The next step involved mapping the reads to both the human genome (GRCh Build

38) and to a comprehensive viral genome database, encompassing over 14,000 distinct viral genomes. This mapping was performed utilizing the ViralTrack software package [18]. Only viral genomes meeting specific criteria were retained for further analysis. These criteria included a minimum coverage of at least 50 reads covering at least 10% of the entire viral genome sequence, and a sequence complexity of 1.3, as indicated by base composition entropy. Viral hits meeting these criteria were then assembled into contigs, which were considered to represent active regions of transcription within the viral genome. Subsequently, only those reads that mapped to contigs with a length of 200 bases or longer were retained. A custom Python script was employed to parse the alignments to both the human and viral genomes. Reads that mapped to both the human genome and a viral genome were assigned to the organism showing the highest alignment score. Finally, the read count of viral hits was quantified for each barcode, and barcodes were categorized as expressing the virus if they contained three or more reads mapped to a viral genome. The resulting viral expression data were integrated into the SingCellaR object for visualization in UMAP projections.

Identification of HERV-K provirus insertion sites

We obtained the genomic coordinates of HERV-K provirus insertions from two previously published sources [20, 138]. Coordinates from the Xue et al. study, originally reported in the hg19 (GRCh37) genome build, were converted to the hg38 (GRCh38) assembly using the liftover Python package (v1.3.2). Coordinates from both studies were then merged and manually curated to remove redundancies. To annotate the genomic context of each insertion, we used GENCODE v44 gene annotations. For each insertion, we recorded overlapping features including gene name, and region type (e.g., exon, intron, intergenic). Using a custom Python script, we quantified read coverage across the merged HERV-K insertion regions using the scRNA-seq data from the three

RE patients, mapped to the reference hg38 (GRCh38) genome build. Reads were considered overlapping if they intersected a given region by at least 10 base pairs. We further filtered reads to retain only those also aligning to a reference HERV-K genome (NC_0022518) as determined from the prior ViralTrack analysis. Additional filtering criteria were applied to reduce mapping artifacts: retained reads were required to have an entropy score ≥ 1.0 , an average Phred-scaled mapping quality ≥ 25 , and a minimum aligned segment length of 20 bases. Chromosomal maps showing the sites of provirus insertion were made using the R package RIdeogram [49].

B cell receptor sequencing

Bulk genomic DNA was isolated from a frozen block of fresh brain tissue from RE patient 738, and from whole blood (Monarch® genomic DNA purification kit, New England Biolabs, Ipswich, MA). BCR sequences were obtained using the ImmunoSEQ® assay (Adaptive Biotechnologies, Seattle, WA), and clonal analysis was performed using the interactive web tool, ViCloD [57].

Immunocytochemistry

Paraffin embedded sections (5 μ m) were stained using Opal Fluorophore reagents (Akoya Biosciences, Marlborough, MA) and a Leica Bond RX auto-stainer (Leica Biosystems, Vista, CA) following antigen retrieval. In one panel, the following antibodies were used: CD20 (Opal 520), HLA-DR (Opal 570), CD4 (Opal 620) CD3 (Opal 690), and CD8 (Opal 780). In a second panel the following two antibodies were used, CD8 (Opal 570), and LAG-3 (Opal 690). Images were collected using a Leica Aperio Versa 200 Slide Scanning Microscope equipped with a 16-bit 5.5-megapixel fluorescence camera, and images were captured using Phenochart 2.0 (Akoya Biosciences), and colors were re-assigned. Images, as Tiff files, were imported into PHOTO-PAINT (Corel Corporation, Ottawa, Canada), to upscale the resolution to 600 dpi, and adjust tone curves. All figures were prepared in CorelDraw (Corel Corporation).

Results

Clinical and Pathological Description

Three RE patients underwent surgery to control their pharmaco-resistant seizures (Table 1 and Fig. S1). In addition to anti-seizure medications (ASMs) two of the patients had received intravenous immunoglobulins (IVIG) in the months prior to surgery. Post-operatively all three patients were seizure free although still taking ASMs. We obtained formalin fixed paraffin sections, blood and fresh brain tissue from the surgical resections. A multiplex immunostaining protocol was used to visualize areas of inflammation in sections of resected brain tissue. Figure 1 shows areas of high HLA-DR expression marking microglia activation, and at higher magnification scattered CD8 and CD4 T cells amidst the activated microglia. In the selected section of brain from patient 738, B cells were intermingled with T cells, and in the case of patient 769 we found a dense cluster of CD4 T cells surrounded by microglia.

Immune cells were isolated from each fresh brain specimen and single cell cDNA libraries were constructed targeting 10,000 cells. Both whole transcriptome and T cell receptor sequences were obtained, and the transcriptomic data from each patient were integrated using canonical correlation analysis (Fig. S2). The identity of the cells in each cluster was assigned based on known marker genes (Fig. S2), and from these assignments, the proportions of the different cell types from the three brain specimens were calculated (Fig. 2). Myeloid cells mainly comprised microglia and were clearly distinguishable from T cells and NK cells, except for a mixed cluster derived primarily from patient 769, which we attribute to cell doublets (Cluster 9, Fig. S2). Cluster 9 cells were excluded from further analysis.

T cell phenotypes

The putative T cells and Natural Killer (NK) cells were extracted from the integrated dataset, and re-clustered to further resolve cell phenotypes (Fig. 3A and B; Table S1). The majority of cells in all 12 clusters expressed CD69 a marker of resident memory T cells (T_{RM}) [26]; a variable number of cells in each cluster also expressed ITGAE (CD103), a second T_{RM} marker [26] (Fig. 3C). Based on differentially expressed genes, three of the 12 clusters contained CD4 T cells, of which cluster 5 was defined by the expression of IL7R and KLRB1, cluster 7 by FOXP3 expression and cluster 9 by KLRB1 and CXCL13 transcripts (Fig. 3C). In agreement with this interpretation GSEA using gene signatures for different T cell phenotypes [111] indicated that cluster 5 contained CD4 memory T cells and cluster 7 comprised regulatory T cells (Tregs) (Table 2). Clusters 1-4, 6 and 10 comprised predominantly CD8 T cells, of which cluster 1 was further defined by high levels of XCL1 transcripts, cluster 3 by GMZK expression, and cluster 6 by high expression of heat shock proteins including HSP1A1 (Fig. 3C). GSEA with gene signatures for T cell phenotypes [111], exhausted T cells [140], and for virus responsive T cells [42] indicated that cluster 1 CD8 T cells had a cytokine producing phenotype and were responsive to a virus whereas cluster 2 and 4 CD8 T cells were likely exhausted. Gamma delta T cells were found within the CD8 T cells clusters; presumably, their overall gene expression profiles were too similar to the alpha beta T cells (Fig. S3). Cluster 8 was defined by a higher level of SKI transcripts, a suppressor of CD103 expression in mice [137], cluster 11 by FCGR3A (CD16) expression, and cluster 12 by XCL1 expression. GSEA with a published Natural killer (NK) cell gene signature [107] indicated that clusters 11 and 12 contained NK cells (Table 2). In addition to the putative NK cells, the majority of CD8 T cells expressed KLRD1 (CD94) mRNA, which encodes an NK cell C-type lectin that forms heterodimers with NKG2 molecules to either inhibit (NKG2A/B) or activate (NKG2C and

NKG2E) NK and CD8 T cells by binding to HLA-E molecules [80]. Higher levels of transcripts encoding the activating receptors were found in the majority of NK cells and CD8 T cells compared with transcripts encoding the inhibitory receptor (Fig. S4). Similarly, *KLRK1* encoding NKG2D, another activating NK cell C-type lectin-like receptor, was also highly expressed whereas *KLRG1* encoding another inhibitory receptor was not (Fig. S4).

Interrogating the dataset for expression of transcripts encoding co-stimulatory and co-inhibitory genes revealed that CD8 T cells expressed the co-stimulatory genes *ICOS*, *CRTAM* and *TNFRSF9*, but essentially no *CD27* or *CD28* (Fig. S5). In contrast to CD4 T cells, *LAG-3* was the dominant co-inhibitory gene expressed by CD8 T cells (Fig. S5); far fewer cells expressed the co-inhibitory gene *PDCD1*, which were largely confined to cluster 9 CD4 T cells. CD4 Tregs (cluster 7) expressed *CTLA4* and *TIGIT* (Fig. S5), as well as the co-stimulatory genes *ICOS*, *TNFRSF9* (4-1BB), *CD27* and *CD28* (Fig. S5). Immunostaining with LAG-3 and CD8 antibodies confirmed the expression of LAG-3 by CD8 T cells (Fig. S6). The intense punctate staining in some CD T cells is consistent with the known intracellular storage of LAG-3 [136]. We also examined the expression of selected transcription factors. More cells expressed *RUNX3*, *ZEB2*, *PRDM1* (Blimp), and *ZNF683* (Hobit) mRNAs than *Tox*, *TBX21* (Tbet) or *TCF7* mRNAs (Fig. S7). However, fewer cells assigned to the CD4 T cell clusters (5, 7 and 9) expressed *ZEB2* and *ZNF683* mRNA compared with cells assigned to the CD8 T cell clusters. Very few cells in the NK cell clusters (11 and 12) expressed *BATF* (Fig. S7).

Clonally focused CD8 T cells

We determined the number of different T cell clonotypes, defined by the Vbeta chain third complementarity region (CDR3) sequence, in the three RE brain specimens (Table S2). From Hill plots, TRBV and TRBJ gene usage, and CDR3 lengths it was clear that T cells in the brains of the

three patients were clonally focused particularly in the brain samples from patients 754 and 769 (Fig. S8). Matching the barcodes from the TCR libraries to those comprising the T cell clusters showed that the most frequent clonotypes (defined as $>1\%$) were found in the CD8 T cell clusters with one exception (Fig. 3D). In patient 769 the most frequent clonotype could be ascribed to cluster 9 corresponding to a CD4 T cell subset defined by the expression of KLRB1 and CXCL13 (Fig. 3E). In patients 738 and 754 the dominant clonotypes were CD8 T cells (Fig. 3E). We confirmed the phenotypes of 49 of the 54 most frequent clonotypes by extracting the CD3D⁺/CD3E⁺ CD4⁺ and CD8⁺ cells (≥ 1 normalized UMI) from the sparse matrix file of the reclustered T cell and NK cells and matching the barcodes to those of the top clonotypes (Table S2). To partition the top 1% into public and private clonotypes we compared them to Adaptive Biotechnologies' immuneACCESS database (Table S2). As shown in Fig. 4 more than half of the abundant clonotypes were public. Vbeta chain CDR3 amino acid sequence and TRBV and TRBJ genes of a rare clonotype in the blood of a single donor from large scale covid study [44] was identical to the most abundant clonotype in patient 754 (Table S3). The CDR3 regions differed by three nucleotides indicating convergent selection [123]. Likewise, the most abundant clonotype in patient 769 was found in five individuals from an unpublished study of celiac disease available in the immuneACCESS database, although TRBV gene usage differed (Table S3).

We compared all the Vbeta CDR3 amino acid sequences to the VDJdb database [11] and found that there were exact matches including TRBV and TRBJ gene usage to TCRs that recognize common viral epitopes. All these matching clonotypes were rare with one exception (Table S4). We implemented ClusTCR [121] to identify clonotypes that may recognize the same epitopes. As shown in Table S5, several clonotypes were found that likely recognize the same antigen, notably HHV4 (IVTDFSVIK), and HHV5 (KLGALQK).

Expansion of B cell clones

We found higher numbers of B cells and antibody-producing plasma cells in the brain specimen from Patient 738 (Figs.1 and 2). Bulk immunoglobulin heavy chain (IGH) sequences were obtained from a fresh frozen piece of tissue from the same surgical specimen, and from whole blood collected at the time of the surgery. Repertoire analysis of IGH sequences identified the six most frequent clones (>1%) in the brain and showed the extent of intra-clonal diversity (Fig. 5). The most abundant clone comprised a single IGH sequence that was not detected in the sample of IGH sequences from the blood suggesting local clonal expansion (Fig. S9).

Myeloid cell phenotypes

Re-clustering the myeloid cells alone generated 14 clusters that were present in different proportions in each patient sample (Fig. 6A and B, Table S6). Pathway analysis associated clusters with different functions and protein complexes based on statistically significant differences in gene expression between clusters (Fig. S10). We interpreted 11 of the clusters as microglia based on the expression of the homeostatic glial marker genes *TMEM119*, *P2RY12*, *OFML3*, *SLC2A5*, and *CXC3CR1* [73, 91, 99] (Fig. 6C). From the analysis of differentially expressed genes, cluster 9 appeared to define a population of macrophages as evidenced by high expression of *CD163* and *FCGR2B* (*CD32*) mRNAs by the majority of cells in the cluster [62, 132] (Fig. 6D). Cells in clusters 10 may comprise a dendritic cell population based on the expression of *CD1c*, *CLEC10A* and *LGALS2* (Galectin-2) whereas cells in cluster 11 appeared to be a monocyte or monocyte-derived population based on *VCAN* (versican) expression [126]. The majority of the cells comprising clusters 9-11 were derived from patient 738 (Fig. 6B).

The microglia populations shared genes expressed by disease-associated microglia, specifically, *TREM2*, *APOE*, *CD83*, and *SPPI* (osteopontin) [52, 73, 75], as well as genes directly

associated with the NPLR3 inflammasome pathway (Fig. 6E) [88, 95]. All myeloid clusters expressed high levels of HLA II molecules (Fig. 6E; see also Fig. 1). Cluster 3 microglia made up the largest fraction of myeloid cells in the brain specimen from Patient 754, whereas cluster 2 microglia were the most abundant myeloid cells in Patient 769 (Fig. 6B). From the differential gene expression analysis, it appeared that cluster 3 microglia expressed higher levels *DNAJB1* and *CCL3* transcripts than cluster 2 microglia, whereas cluster 2 microglia expressed higher levels of *AIF1* (IB1A), and *FCGR3A* (CD16) mRNA (Fig. 6F). Less granular clustering of the myeloid cells and trajectory analysis using Monocle 3.0 indicated that microglia cells may transition from CD83⁻ cells expressing more IBA1 and CD16 to CD83⁺ cells expressing cytokines and heat shock proteins (Figure S11 and Table S7).

Predicted myeloid cell: T cell communication

We implemented LIANA+ to investigate potential binding of ligands expressed by microglia and monocyte derived cells (Fig. 6D) to cognate receptors on T cells and NK cells. The results of this analysis are shown in Table S8 in which the same ligand: receptor pairings are highly ranked by seven different methods (see Methods and Materials for details). Microglia and monocyte-derived cells were predicted to interact with T cells (and NK cells) via ligand binding to several co-stimulatory and co-inhibitory receptors (Fig. 7). One of the strongest predictions as evidenced by the high specificity and magnitude rankings involved HLA class II proteins on myeloid cells and the co-inhibitory receptor LAG-3 on T cells/NK cells [21]. Galectin-3, encoded by *LGALS3*, and expressed by monocyte-derived cells was also predicted to bind LAG-3 [21]. In addition, CD86 and CD80 binding to a second co-inhibitory receptor, CTLA, may also regulate T cell activity [47]. For microglia the SPP1: CD44 ligand: receptor pairing was ranked the highest. It has been reported that SPP1 (osteonectin) binding to CD44 suppresses T cell activation [63].

The LIANA+ analysis also highlighted potential activating interactions between myeloid cells and T cells and NK cells involving CD2, CD6, CD226, CRTAM, and TNFRSF9 (4-1BB) [15, 17, 27, 55, 131]. The CD226 ligand Netrin-2 also binds the co-inhibitory receptor TIGIT [58], which we found was predominantly expressed by Tregs (Fig. S5). This interaction was not predicted probably because the number of TIGIT⁺ T cells did not meet the threshold that at least 20% of cells express the ligand or receptor gene. The expression of ligand genes in each myeloid cluster and the corresponding receptor genes in T cells and NK cells is shown in Fig. S12.

Endogenous HERVK activation

We used ViralTrack [18] to search for viral transcripts in the scRNA-seq data from each RE brain specimen. Based on the filtering steps applied in the analysis (see Methods and Materials) we did not find evidence for any active exogenous viruses in the dataset. However, we did find evidence for activity of the endogenous retrovirus, HERV-K. The filtered HERV-K reads from each RE case could be uniquely mapped to previously identified sites of provirus insertion [20, 138] (Fig. 8; Table S9), indicating that multiple copies of HERV-K were transcriptionally active. Out of a total of 49 proviruses, 11 were in common between the three RE cases, and 13 were previously shown to be active in normal brain [20]. Associating reads with individual barcodes and imposing a threshold of at least three reads per barcode showed that HERV-K was active in more immune cells from patient 754 compared with the other two patients (Fig. S13). As shown in Figure 8, the highest number of active proviruses was found in patient 754.

Discussion

We have used scRNA-seq to characterize the immune landscape in brain areas affected by RE from three hemispherectomy surgery cases. The ages of the three patients, their treatment and

timing of surgery were different, nevertheless it was possible to find the same types of immune cells in the resected brain tissue from each patient. Based on CD69 and CD103 antibody staining of T cells from other RE cases we previously reported that the majority of T cells in resected brain tissue were $T_{RM}s$ indicating that they had entered the brain at an earlier time point before the surgery in response to an immune challenge, and then had remained there [86]. In the present study we found that essentially all CD4 and CD8 T cells and NK cells expressed CD69 and variable levels of ITGAE (CD103) mRNA. We also documented the expression RUNX3, PRDM1 (Blimp-1), and ZNF683 (Hobit), transcription factors that have been implicated in establishing $T_{RM}s$ [41, 70].

The bioinformatics pipeline that we employed identified distinct populations of CD4 and CD8 T cells. The major CD8 T cell populations, which accounted for most of the high frequency clonotypes, comprised cells that expressed genes associated with an effector phenotype, as evidenced by the expression of the granzyme gene *GZMB*, and the NK cell activating C-type lectin-like genes *KRLD2*, *KLRKC2*, *KLRC3* and *KLRK1*. We also detected a population of CD8 T cells characterized by high levels of *GZMK* transcripts. Unlike Granzyme B, Granzyme K can induce non-caspase dependent cell death by cleaving both cytotoxic and non-cytotoxic intracellular proteins [19]. $GZMK^+$ CD8 T cells have been found in tissues and lesions associated with several different autoimmune diseases and are assumed to be autoreactive [6, 61].

Exhausted T cells have been extensively described in chronic infections and cancers [79] and are characterized by high expression of co-inhibitory molecules including PD1, LAG-3, TIM-3, and TIGIT [10]. The persistence of disease-triggering self-antigens in autoimmune diseases is also expected to generate an exhausted or dysfunctional state. GSEA indicated that there were exhausted T cells among the CD8 T cells found in affected RE brain tissue; notably LAG-3

transcripts were detected in about half the CD8 cells. We confirmed that LAG-3⁺ CD8 T cells were present in a section of resected brain tissue, consonant with a recent report [71]. In this study it was found that the number of T cells expressing PD-1 was significantly higher in tissue sections from later clinical stages compared with early stages of the disease, potentially reflecting an increase in the proportion of exhausted T cells. This difference between clinical stages could explain why we found few T cells expressing PD-1 transcripts in our dataset. In a mouse model of type 1 diabetes, it was shown that LAG-3⁺ intra-islet CD8 T cells had an exhausted-like phenotype [45]. Deleting *Lag3* accelerated the development of diabetes, strongly implicating LAG-3⁺ CD8 T cells in the disease [13]. LAG-3 binds HLA class II molecules, and also binds to other ligands including the product of the *LGALS3* gene, Galectin 3 [21]. We found HLA class II transcripts in essentially all myeloid cells, and LIANA+ predicted a specific interaction with LAG-3⁺ T cells, and also between LAG-3 and Galectin-3 on monocyte-derived cell, which suggests that the effector function of CD8 T cells might be held in check by these interactions. A LAG-3 agonist antibody has been developed as a potential treatment for autoimmune diseases [5]. An immunosuppressive interaction between microglia and T cells and NK cells may also involve osteopontin binding to CD44 [63]. *SSP1* and *CD44* genes were expressed in the majority of microglia and T cells and NK cells respectively.

There are a number of reports documenting the presence of active HHV4 and HHV5 in brain areas affected in RE [69, 94, 127]. We found exact HLA-matched TRB sequences in the three RE brain specimens that have been shown to recognize immunodominant peptides from HHV4 and HHV5 indicating that the three patients may have been exposed to these viruses leading to a subclinical immune response and viral latency in circulating monocytes and B cells [9, 100, 108]. Although the HHV4 and HHV5-specific T cell clonotypes did not correspond to the most abundant

clonotypes in each surgery case, we considered the possibility that a reactivated herpes virus was present in peripheral immune cells present in the brain [98]. We used ViralTrack to search for viral transcripts in our dataset but did not find any herpes virus transcripts. We cannot exclude the possibility of an active virus in other brain cells or that infected cells had already been eliminated leaving behind resident memory T cells [128].

Over half of the frequent clonotypes (>1%) were public suggesting that some of the expanded T cells in the brain might result from exposure to a common infectious agent, and raising the possibility of molecular mimicry if these T cells also recognize self-antigens [112]. In patient 769 the Vbeta CDR3 amino acid sequence of the most abundant clonotype only matched a rare clonotype in the blood of seven individuals diagnosed with celiac disease, and in patient 754 the Vbeta CDR3 sequence and TRB and TRJ genes exactly matched a rare clonotype in the blood of a single uninfected individual from a recent SARS-CoV-2 study (Table S3) [44]. Given the limited sharing of these two clonotypes with other individuals it is possible that they may have escaped peripheral tolerance mechanisms and be directly autoreactive.

In our search for viral transcripts, we found HERV-K sequences in our scRNA-seq data indicating that this endogenous retrovirus was activated in immune cells from each RE patient. Mapping the virus contigs in individual cells showed that more microglia expressed HERV-K in patient 754 than in the other two patients. It has been reported that the presence of HERV-K transcripts in glioblastomas, teratoid rhabdoid tumors and in spinal cord neurons of ALS patients has potential disease-modifying effects [34, 90, 106]. Among the eleven proviruses active in all three patients, the provirus at Chr7p22.1a, ERK-6 (HERV-K108) contains full length open reading frames for the gagpol and envelope (env) genes; a mutation in the reverse transcriptase domain renders the virus defective [76]. The envelope gene from this provirus has been shown to be

translated and expressed on the cell surface of transfected cells [30]. Whether the env protein is expressed in affected brain areas in RE remains to be determined. It has been reported that a GU-rich sequence in the env gene RNA can trigger TLR8-dependent death of neurons indicating that any pathological consequence of HERV-K activation might not depend on a translated open reading frame [29]. We should note that HERV-K sequences, including 13 we identified in the RE specimens, have also been found in transcript data from normal brain samples in the GTEx database including ERK-6 [20, 82].

CD4 T cells could be assigned to three different phenotypes Tregs, IL7R⁺ memory cells, and a population of T cells distinguished by the expression of CXCL13 and KLRB1 (CD161) transcripts. CXCL13 is a chemoattractant for B cells, and CD4 cells producing this cytokine have been associated with the formation of tertiary lymphoid structures (TLS) [120]. In Fig. 1, a cluster of CD4⁺ T cells surrounded by HLA-DR⁺ myeloid cells could correspond to this CD4 T cell subtype and define a developing TLS. Such ectopic structures have been found in affected tissues in autoimmune diseases [93], and CD4 T cells producing CXCL13 are present in synovial fluid in Rheumatoid arthritis patients [64]. In Patient 769 the most frequent clonotype was in fact this CD4 T cell subtype (Table S2). On the other hand, we found the highest number of B cells and plasma cells in Patient 738. A higher number of monocyte-derived cells was also present in the sample of brain tissue from this patient. Sequencing immunoglobulin heavy chains revealed that these cells comprised expanded clones implying a specific humoral response to an antigen(s) in the brain of this patient. Patient 738 was the oldest surgery case at 26 years old, and seizure onset was documented five years earlier according to his clinical history (Table 1). However, the patient also experienced seizures when he was four years old and was treated with ASMs for two years. We speculate that the onset of seizures later in life may reflect a reactivation of resident T cells and a

de novo humoral response. Autoantibodies directed against synaptic proteins have been found in the blood from some RE patients [3, 83, 139], which has led to the use of an anti-CD20 antibody to try to control the disease [36, 56, 116, 117].

TIGIT expression by Tregs suggested that they were likely to be highly suppressive effector Tregs [60]. Therefore, their presence in the affected areas of the brain may play a pivotal role in suppressing the activity of the clonally focused CD8 T cells found in the same brain areas. It has been proposed that Treg dysfunction contributes to the etiology of autoimmune diseases [81, 110], and ways to increase Treg numbers and efficacy in autoimmune diseases are being actively pursued [81, 102, 105]. In addition to TIGIT, our analysis indicated that Tregs were regulated by several other co-stimulatory and co-inhibitory proteins including ICOS, CD27, CD28, and CTLA4 (Figure S6). CTLA4 is constitutively expressed by Tregs and competes with CD28 for binding to CD86 and CD80 on antigen presenting cells to suppress conventional T cells by cell intrinsic and extrinsic mechanisms [125, 134], that may also involve engagement of the TCR [31]. We detected CD86 transcripts in the majority of myeloid cells and CD80 transcripts in monocyte-derived cells. LIANA+ predicted binding to CTLA4 suggesting that myeloid cells may regulate Treg cells present in the affected brain area via CTLA4 binding to CD80 and CD86 [47].

Most of myeloid cells that we isolated from affected brain tissue were microglia and were distinguished from smaller populations of macrophages and monocyte-derived immune cells (monocyte-derived macrophages and monocyte-derived dendritic cells). Based on the default resolution parameter used, ten clusters of microglia were generated by the Louvain algorithm, although all cells expressed known homeostatic microglia marker genes, and genes associated with activated microglia. Trajectory analysis indicated that microglia transitioned from cells expressing higher transcript levels of genes associated with phagocytosis, FCGR3A (CD16) and AIF1 (Ib1a),

to cells expressing higher levels of proinflammatory cytokines, CCL3/4 and CD83 and to cells expressing CD83, cytokine and heat shock protein transcripts, although the latter might be attributable to stress induced during *ex vivo* dissociation of the brain tissue [72]. On the other hand, a subpopulation of microglia characterized by CD83 and heat shock protein gene expression was found to be selectively depleted in the substantia nigra of Parkinson disease patients implying a protective function that may also pertain to RE [24].

Most microglia expressed HLA class II molecules, ITAGX (CD11c), and CD86 transcripts indicating competency as antigen presenting cells [25, 101]. As previously discussed, microglia could regulate CD8 T cell activity via LAG-3 binding to HLA class II molecules. In a mouse model of type 1 diabetes, a *Lag3* mutation that disrupts binding to stable MHC II causes the same disease exacerbation as a *Lag3* null mutation[74].

Conclusion

Our analysis highlights the complexity of the immune landscape in brain areas affected by RE and supports the involvement of clonally expanded antigen experienced resident memory CD8 T cells in the etiology of RE. The presence of resident CD4 Tregs in the affected brain area suggests that they may be playing a role in restraining the activity of the conventional T cells. Likewise, microglia and monocyte-derived cells may regulate T cell activity via co-inhibitory and co-stimulatory receptor binding. However, further work involving expanded multiplex antibody panels and spatial analysis will be necessary to validate predictions of ligand: receptor binding between myeloid cells and T cells based on the mRNA expression data. Activation of HERV-K proviruses in the affected brain area may be unrelated to the etiology of RE although it is

conceivable that translation of viral proteins from this endogenous virus could generate neo-antigens to which the patient's immune system may react.

References

- 1 Ai J, Wang Y, Liu D, Fan D, Wang Q, Li T, Luan G, Wang P, An J (2021) Genetic Factors in Rasmussen's Encephalitis Characterized by Whole-Exome Sequencing. *Front Neurosci* 15: 744429 Doi 10.3389/fnins.2021.744429
- 2 Al Nimer F, Jelcic I, Kempf C, Pieper T, Budka H, Sospedra M, Martin R (2018) Phenotypic and functional complexity of brain-infiltrating T cells in Rasmussen encephalitis. *Neurol Neuroimmunol Neuroinflamm* 5: e419 Doi 10.1212/NXI.0000000000000419
- 3 Alvarez-Baron E, Bien CG, Schramm J, Elger CE, Becker AJ, Schoch S (2008) Autoantibodies to Munc18, cerebral plasma cells and B-lymphocytes in Rasmussen encephalitis. *Epilepsy Res* 80: 93-97 Doi 10.1016/j.epilepsyres.2008.03.007
- 4 Amrom D, Kinay D, Hart Y, Berkovic SF, Laxer K, Andermann F, Andermann E, Bar-Or A (2014) Rasmussen encephalitis and comorbid autoimmune diseases: A window into disease mechanism? *Neurology* 83: 1049-1055 Doi 10.1212/WNL.0000000000000791
- 5 Angin M, Brignone C, Triebel F (2020) A LAG-3-Specific Agonist Antibody for the Treatment of T Cell-Induced Autoimmune Diseases. *J Immunol* 204: 810-818 Doi 10.4049/jimmunol.1900823
- 6 Arazi A, Rao DA, Berthier CC, Davidson A, Liu Y, Hoover PJ, Chicoine A, Eisenhaure TM, Jonsson AH, Li Set al (2019) The immune cell landscape in kidneys of patients with lupus nephritis. *Nat Immunol* 20: 902-914 Doi 10.1038/s41590-019-0398-x

- 7 Asgrimsdottir ES, Bassini LF, Sun T, Puigsasllosas Pastor C, di Val Cervo PR, Gyllborg D, Lee K, Grigsby CL, Jude B, Abaurre Cet al (2026) Distinct radial glia subtypes regulate midbrain dopaminergic neuron development. *Nat Neurosci*: Doi 10.1038/s41593-026-02200-8
- 8 Atkins MR, Terrell W, Hulette CM (1995) Rasmussen's syndrome: a study of potential viral etiology. *Clin Neuropathol* 14: 7-12
- 9 Babcock GJ, Decker LL, Volk M, Thorley-Lawson DA (1998) EBV persistence in memory B cells in vivo. *Immunity* 9: 395-404 Doi 10.1016/s1074-7613(00)80622-6
- 10 Baessler A, Vignali DAA (2024) T Cell Exhaustion. *Annu Rev Immunol* 42: 179-206 Doi 10.1146/annurev-immunol-090222-110914
- 11 Bagaev DV, Vroomans RMA, Samir J, Stervbo U, Rius C, Dolton G, Greenshields-Watson A, Attaf M, Egorov ES, Zvyagin IVet al (2020) VDJdb in 2019: database extension, new analysis infrastructure and a T-cell receptor motif compendium. *Nucleic Acids Res* 48: D1057-D1062 Doi 10.1093/nar/gkz874
- 12 Bast T, Ramantani G, Seitz A, Rating D (2006) Focal cortical dysplasia: prevalence, clinical presentation and epilepsy in children and adults. *Acta Neurol Scand* 113: 72-81 Doi 10.1111/j.1600-0404.2005.00555.x
- 13 Bettini M, Szymczak-Workman AL, Forbes K, Castellaw AH, Selby M, Pan X, Drake CG, Korman AJ, Vignali DA (2011) Cutting edge: accelerated autoimmune diabetes in the absence of LAG-3. *J Immunol* 187: 3493-3498 Doi 10.4049/jimmunol.1100714
- 14 Bien CG, Granata T, Antozzi C, Cross JH, Dulac O, Kurthen M, Lassmann H, Mantegazza R, Villemure JG, Spreafico Ret al (2005) Pathogenesis, diagnosis and treatment of Rasmussen encephalitis: a European consensus statement. *Brain* 128: 454-471

- 15 Binder C, Cvetkovski F, Sellberg F, Berg S, Paternina Visbal H, Sachs DH, Berglund E, Berglund D (2020) CD2 Immunobiology. *Front Immunol* 11: 1090 Doi 10.3389/fimmu.2020.01090
- 16 Bjornevik K, Munz C, Cohen JI, Ascherio A (2023) Epstein-Barr virus as a leading cause of multiple sclerosis: mechanisms and implications. *Nat Rev Neurol* 19: 160-171 Doi 10.1038/s41582-023-00775-5
- 17 Boles KS, Barchet W, Diacovo T, Cella M, Colonna M (2005) The tumor suppressor TSLC1/NECL-2 triggers NK-cell and CD8+ T-cell responses through the cell-surface receptor CRTAM. *Blood* 106: 779-786 Doi 10.1182/blood-2005-02-0817
- 18 Bost P, Giladi A, Liu Y, Bendjelal Y, Xu G, David E, Blecher-Gonen R, Cohen M, Medaglia C, Li Het al (2020) Host-Viral Infection Maps Reveal Signatures of Severe COVID-19 Patients. *Cell* 181: 1475-1488 e1412 Doi 10.1016/j.cell.2020.05.006
- 19 Bouwman AC, van Daalen KR, Crnko S, Ten Broeke T, Bovenschen N (2021) Intracellular and Extracellular Roles of Granzyme K. *Front Immunol* 12: 677707 Doi 10.3389/fimmu.2021.677707
- 20 Burn A, Roy F, Freeman M, Coffin JM (2022) Widespread expression of the ancient HERV-K (HML-2) provirus group in normal human tissues. *PLoS Biol* 20: e3001826 Doi 10.1371/journal.pbio.3001826
- 21 Burnell SEA, Capitani L, MacLachlan BJ, Mason GH, Gallimore AM, Godkin A (2022) Seven mysteries of LAG-3: a multi-faceted immune receptor of increasing complexity. *Immunother Adv* 2: ltab025 Doi 10.1093/immadv/ltab025

- 22 Cabello-Aguilar S, Alame M, Kon-Sun-Tack F, Fau C, Lacroix M, Colinge J (2020) SingleCellSignalR: inference of intercellular networks from single-cell transcriptomics. *Nucleic Acids Res* 48: e55 Doi 10.1093/nar/gkaa183
- 23 Cao J, Spielmann M, Qiu X, Huang X, Ibrahim DM, Hill AJ, Zhang F, Mundlos S, Christiansen L, Steemers FJ et al (2019) The single-cell transcriptional landscape of mammalian organogenesis. *Nature* 566: 496-502 Doi 10.1038/s41586-019-0969-x
- 24 Chatila ZK, Yadav A, Mares J, Flowers X, Yun TD, Rashid M, Talcoff R, Pelly Z, Zhang Y, De Jager P et al (2023) RNA- and ATAC-sequencing Reveals a Unique CD83+ Microglial Population Focally Depleted in Parkinson's Disease. *bioRxiv*: Doi 10.1101/2023.05.17.540842
- 25 Chhatbar C, Prinz M (2021) The roles of microglia in viral encephalitis: from sense to therapeutic targeting. *Cell Mol Immunol* 18: 250-258 Doi 10.1038/s41423-020-00620-5
- 26 Christo SN, Park SL, Mueller SN, Mackay LK (2024) The Multifaceted Role of Tissue-Resident Memory T Cells. *Annu Rev Immunol* 42: 317-345 Doi 10.1146/annurev-immunol-101320-020220
- 27 Consuegra-Fernandez M, Lin F, Fox DA, Lozano F (2018) Clinical and experimental evidence for targeting CD6 in immune-based disorders. *Autoimmun Rev* 17: 493-503 Doi 10.1016/j.autrev.2017.12.004
- 28 Dandekar S, Wijesuriya H, Geiger T, Hamm D, Mathern GW, Owens GC (2016) Shared HLA Class I and II Alleles and Clonally Restricted Public and Private Brain-Infiltrating alpha-beta T Cells in a Cohort of Rasmussen Encephalitis Surgery Patients. *Front Immunol* 7: 608 Doi 10.3389/fimmu.2016.00608

- 29 Dembny P, Newman AG, Singh M, Hinz M, Szczepek M, Kruger C, Adalbert R, Dzaye O, Trimbuch T, Wallach Tet al (2020) Human endogenous retrovirus HERV-K(HML-2) RNA causes neurodegeneration through Toll-like receptors. *JCI Insight* 5: Doi 10.1172/jci.insight.131093
- 30 Dewannieux M, Blaise S, Heidmann T (2005) Identification of a functional envelope protein from the HERV-K family of human endogenous retroviruses. *J Virol* 79: 15573-15577 Doi 10.1128/JVI.79.24.15573-15577.2005
- 31 Dikiy S, Rudensky AY (2023) Principles of regulatory T cell function. *Immunity* 56: 240-255 Doi 10.1016/j.immuni.2023.01.004
- 32 Dimitrov D, Schafer PSL, Farr E, Rodriguez-Mier P, Lobentanzer S, Badia IMP, Dugourd A, Tanevski J, Ramirez Flores RO, Saez-Rodriguez J (2024) LIANA+ provides an all-in-one framework for cell-cell communication inference. *Nat Cell Biol* 26: 1613-1622 Doi 10.1038/s41556-024-01469-w
- 33 Dimitrov D, Turei D, Garrido-Rodriguez M, Burmedi PL, Nagai JS, Boys C, Ramirez Flores RO, Kim H, Szalai B, Costa IGet al (2022) Comparison of methods and resources for cell-cell communication inference from single-cell RNA-Seq data. *Nat Commun* 13: 3224 Doi 10.1038/s41467-022-30755-0
- 34 Doucet-O'Hare TT, DiSanza BL, DeMarino C, Atkinson AL, Rosenblum JS, Henderson LJ, Johnson KR, Kowalak J, Garcia-Montojo M, Allen SJet al (2021) SMARCB1 deletion in atypical teratoid rhabdoid tumors results in human endogenous retrovirus K (HML-2) expression. *Sci Rep* 11: 12893 Doi 10.1038/s41598-021-92223-x

- 35 Efremova M, Vento-Tormo M, Teichmann SA, Vento-Tormo R (2020) CellPhoneDB: inferring cell-cell communication from combined expression of multi-subunit ligand-receptor complexes. *Nat Protoc* 15: 1484-1506 Doi 10.1038/s41596-020-0292-x
- 36 Erdogan S, Aliyeva G, Kizil TEO, Sener O (2024) Rituximab-responsive late-onset Rasmussen's encephalitis. *Seizure* 123: 57-59 Doi 10.1016/j.seizure.2024.10.009
- 37 Eugster A, Lorenc A, Kotrulev M, Kamra Y, Goel M, Steinberg-Bains K, Sabbah S, Dietz S, Bonifacio E, Peakman Met al (2024) Physiological and pathogenic T cell autoreactivity converge in type 1 diabetes. *Nat Commun* 15: 9204 Doi 10.1038/s41467-024-53255-9
- 38 Farrell MA, Cheng L, Cornford ME, Grody WW, Vinters HV (1991) Cytomegalovirus and Rasmussen's encephalitis. *Lancet* 337: 1551-1552
- 39 Fauser S, Elger CE, Woermann F, Bien CG (2022) Rasmussen encephalitis: Predisposing factors and their potential role in unilaterality. *Epilepsia* 63: 108-119 Doi 10.1111/epi.17131
- 40 Flor M (2020) R interface to D3 chord diagrams <https://github.com/mattflor/chorddiag>
- 41 Fonseca R, Burn TN, Gandolfo LC, Devi S, Park SL, Obers A, Evrard M, Christo SN, Buquicchio FA, Lareau CAet al (2022) Runx3 drives a CD8(+) T cell tissue residency program that is absent in CD4(+) T cells. *Nat Immunol* 23: 1236-1245 Doi 10.1038/s41590-022-01273-4
- 42 Fuchs YF, Sharma V, Eugster A, Kraus G, Morgenstern R, Dahl A, Reinhardt S, Petzold A, Lindner A, Lobel Det al (2019) Gene Expression-Based Identification of Antigen-Responsive CD8(+) T Cells on a Single-Cell Level. *Front Immunol* 10: 2568 Doi 10.3389/fimmu.2019.02568

- 43 Galev G, Prayson RA (2024) Focal cortical dysplasia is a frequent coexistent pathology in patients with Rasmussen's encephalitis. *Ann Diagn Pathol* 68: 152224 Doi 10.1016/j.anndiagpath.2023.152224
- 44 Gittelman RM, Lavezzo E, Snyder TM, Zahid HJ, Carty CL, Elyanow R, Dalai S, Kirsch I, Baldo L, Manuto Let al (2022) Longitudinal analysis of T cell receptor repertoires reveals shared patterns of antigen-specific response to SARS-CoV-2 infection. *JCI Insight* 7: Doi 10.1172/jci.insight.151849
- 45 Grebinoski S, Zhang Q, Cillo AR, Manne S, Xiao H, Brunazzi EA, Tabib T, Cardello C, Lian CG, Murphy GF et al (2022) Autoreactive CD8(+) T cells are restrained by an exhaustion-like program that is maintained by LAG3. *Nat Immunol* 23: 868-877 Doi 10.1038/s41590-022-01210-5
- 46 Hagberg H, Mallard C, Ferriero DM, Vannucci SJ, Levison SW, Vexler ZS, Gressens P (2015) The role of inflammation in perinatal brain injury. *Nat Rev Neurol* 11: 192-208 Doi 10.1038/nrneurol.2015.13
- 47 Halliday N, Williams C, Kennedy A, Waters E, Pesenacker AM, Soskic B, Hinze C, Hou TZ, Rowshanravan B, Janman Det al (2020) CD86 Is a Selective CD28 Ligand Supporting FoxP3+ Regulatory T Cell Homeostasis in the Presence of High Levels of CTLA-4. *Front Immunol* 11: 600000 Doi 10.3389/fimmu.2020.600000
- 48 Hao Y, Hao S, Andersen-Nissen E, Mauck WM, 3rd, Zheng S, Butler A, Lee MJ, Wilk AJ, Darby C, Zager Met al (2021) Integrated analysis of multimodal single-cell data. *Cell* 184: 3573-3587 e3529 Doi 10.1016/j.cell.2021.04.048

- 49 Hao Z, Lv D, Ge Y, Shi J, Weijers D, Yu G, Chen J (2020) RIdiogram: drawing SVG graphics to visualize and map genome-wide data on the idiograms. *PeerJ Comput Sci* 6: e251 Doi 10.7717/peerj-cs.251
- 50 Harris WB, Phillips HW, Chen JS, Weil AG, Ibrahim GM, Fallah A (2020) Seizure outcomes in children with Rasmussen's encephalitis undergoing resective or hemispheric epilepsy surgery: an individual participant data meta-analysis. *J Neurosurg Pediatr* 25: 274-283 Doi 10.3171/2019.9.PEDS19380
- 51 Hart YM, Andermann F, Robitaille Y, Laxer KD, Rasmussen T, Davis R (1998) Double pathology in Rasmussen's syndrome: a window on the etiology? *Neurology* 50: 731-735
- 52 Holtman IR, Raj DD, Miller JA, Schaafsma W, Yin Z, Brouwer N, Wes PD, Moller T, Orre M, Kamphuis Wet al (2015) Induction of a common microglia gene expression signature by aging and neurodegenerative conditions: a co-expression meta-analysis. *Acta Neuropathol Commun* 3: 31 Doi 10.1186/s40478-015-0203-5
- 53 Hou R, Denisenko E, Ong HT, Ramilowski JA, Forrest ARR (2020) Predicting cell-to-cell communication networks using NATMI. *Nat Commun* 11: 5011 Doi 10.1038/s41467-020-18873-z
- 54 Hsieh TC, Ma, K. H., Chao, A. (2016) iNEXT: an R package for rarefaction and extrapolation of species diversity (Hill numbers). *Methods in Ecology and Evolution* 7: 1451-1456
- 55 Huang Z, Qi G, Miller JS, Zheng SG (2020) CD226: An Emerging Role in Immunologic Diseases. *Front Cell Dev Biol* 8: 564 Doi 10.3389/fcell.2020.00564

- 56 Jagtap SA, Patil S, Joshi A, Kurwale N, Jain V, Deshmukh Y (2022) Rituximab in Rasmussen's encephalitis: A single center experience and review of the literature. *Epilepsy Behav Rep* 19: 100540 Doi 10.1016/j.ebr.2022.100540
- 57 Jeusset L, Abdollahi N, Verny T, Armand M, De Septenville AL, Davi F, Bernardes JS (2023) ViCloD, an interactive web tool for visualizing B cell repertoires and analyzing intraclonal diversities: application to human B-cell tumors. *NAR Genom Bioinform* 5: lqad064 Doi 10.1093/nargab/lqad064
- 58 Jin HS, Park Y (2021) Hitting the complexity of the TIGIT-CD96-CD112R-CD226 axis for next-generation cancer immunotherapy. *BMB Rep* 54: 2-11 Doi 10.5483/BMBRep.2021.54.1.229
- 59 Jin S, Guerrero-Juarez CF, Zhang L, Chang I, Ramos R, Kuan CH, Myung P, Plikus MV, Nie Q (2021) Inference and analysis of cell-cell communication using CellChat. *Nat Commun* 12: 1088 Doi 10.1038/s41467-021-21246-9
- 60 Joller N, Lozano E, Burkett PR, Patel B, Xiao S, Zhu C, Xia J, Tan TG, Sefik E, Yajnik V et al (2014) Treg cells expressing the coinhibitory molecule TIGIT selectively inhibit proinflammatory Th1 and Th17 cell responses. *Immunity* 40: 569-581 Doi 10.1016/j.immuni.2014.02.012
- 61 Jonsson AH, Zhang F, Dunlap G, Gomez-Rivas E, Watts GFM, Faust HJ, Rupani KV, Mears JR, Meednu N, Wang R et al (2022) Granzyme K(+) CD8 T cells form a core population in inflamed human tissue. *Sci Transl Med* 14: eabo0686 Doi 10.1126/scitranslmed.abo0686
- 62 Kim WK, Alvarez X, Fisher J, Bronfin B, Westmoreland S, McLaurin J, Williams K (2006) CD163 identifies perivascular macrophages in normal and viral encephalitic brains and

- potential precursors to perivascular macrophages in blood. *Am J Pathol* 168: 822-834 Doi 10.2353/ajpath.2006.050215
- 63 Klement JD, Paschall AV, Redd PS, Ibrahim ML, Lu C, Yang D, Celis E, Abrams SI, Ozato K, Liu K (2018) An osteopontin/CD44 immune checkpoint controls CD8⁺ T cell activation and tumor immune evasion. *J Clin Invest* 128: 5549-5560 Doi 10.1172/JCI123360
- 64 Kobayashi S, Murata K, Shibuya H, Morita M, Ishikawa M, Furu M, Ito H, Ito J, Matsuda S, Watanabe Tet al (2013) A distinct human CD4⁺ T cell subset that secretes CXCL13 in rheumatoid synovium. *Arthritis Rheum* 65: 3063-3072 Doi 10.1002/art.38173
- 65 Kolde R, Laur S, Adler P, Vilo J (2012) Robust rank aggregation for gene list integration and meta-analysis. *Bioinformatics* 28: 573-580 Doi 10.1093/bioinformatics/btr709
- 66 Korsunsky I, Millard N, Fan J, Slowikowski K, Zhang F, Wei K, Baglaenko Y, Brenner M, Loh PR, Raychaudhuri S (2019) Fast, sensitive and accurate integration of single-cell data with Harmony. *Nat Methods* 16: 1289-1296 Doi 10.1038/s41592-019-0619-0
- 67 Kumar P, Lim A, Hazirah SN, Chua CJH, Ngoh A, Poh SL, Yeo TH, Lim J, Ling S, Sutamam NBet al (2022) Single-cell transcriptomics and surface epitope detection in human brain epileptic lesions identifies pro-inflammatory signaling. *Nat Neurosci* 25: 956-966 Doi 10.1038/s41593-022-01095-5
- 68 Leitner DF, Lin Z, Sawaged Z, Kanshin E, Friedman D, Devore S, Ueberheide B, Chang JW, Mathern GW, Anink JJet al (2023) Brain molecular mechanisms in Rasmussen encephalitis. *Epilepsia* 64: 218-230 Doi 10.1111/epi.17457
- 69 Liu D, Wang X, Wang Y, Wang P, Fan D, Chen S, Guan Y, Li T, An J, Luan G (2018) Detection of EBV and HHV6 in the Brain Tissue of Patients with Rasmussen's Encephalitis. *Virolog Sin* 33: 402-409 Doi 10.1007/s12250-018-0063-9

- 70 Mackay LK, Minnich M, Kragten NA, Liao Y, Nota B, Seillet C, Zaid A, Man K, Preston S, Freestone Det al (2016) Hobit and Blimpl1 instruct a universal transcriptional program of tissue residency in lymphocytes. *Science* 352: 459-463 Doi 10.1126/science.aad2035
- 71 Mair KM, Guggenberger V, Verdu de Juan L, Kock U, Lassmann H, Liblau RS, Bien CG, Bauer J (2025) The dynamics of brain T cell populations during the course of rasmussen encephalitis: from expansion to exhaustion. *J Neuroinflammation* 22: 155 Doi 10.1186/s12974-025-03477-5
- 72 Marsh SE, Walker AJ, Kamath T, Dissing-Olesen L, Hammond TR, de Soysa TY, Young AMH, Murphy S, Abdulraouf A, Nadaf Net al (2022) Dissection of artifactual and confounding glial signatures by single-cell sequencing of mouse and human brain. *Nat Neurosci* 25: 306-316 Doi 10.1038/s41593-022-01022-8
- 73 Martins-Ferreira R, Calafell-Segura J, Leal E, Rodriguez-Ubreva J, Martinez-Saez E, Mereu E, Pinho ECP, Laguna A, Ballestar E (2025) The Human Microglia Atlas (HuMicA) unravels changes in disease-associated microglia subsets across neurodegenerative conditions. *Nat Commun* 16: 739 Doi 10.1038/s41467-025-56124-1
- 74 Maruhashi T, Sugiura D, Okazaki IM, Shimizu K, Maeda TK, Ikubo J, Yoshikawa H, Maenaka K, Ishimaru N, Kosako Het al (2022) Binding of LAG-3 to stable peptide-MHC class II limits T cell function and suppresses autoimmunity and anti-cancer immunity. *Immunity* 55: 912-924 e918 Doi 10.1016/j.immuni.2022.03.013
- 75 Masuda T, Sankowski R, Staszewski O, Prinz M (2020) Microglia Heterogeneity in the Single-Cell Era. *Cell Rep* 30: 1271-1281 Doi 10.1016/j.celrep.2020.01.010

- 76 Mayer J, Sauter M, Racz A, Scherer D, Mueller-Lantsch N, Meese E (1999) An almost-intact human endogenous retrovirus K on human chromosome 7. *Nat Genet* 21: 257-258
Doi 10.1038/6766
- 77 McLachlan RS, Diosy D, Levin S (2011) Early treatment of a progressive Rasmussen's like syndrome with ganciclovir. *Can J Neurol Sci* 38: 296-298
- 78 McLachlan RS, Levin S, Blume WT (1996) Treatment of Rasmussen's syndrome with ganciclovir. *Neurology* 47: 925-928
- 79 McLane LM, Abdel-Hakeem MS, Wherry EJ (2019) CD8 T Cell Exhaustion During Chronic Viral Infection and Cancer. *Annu Rev Immunol* 37: 457-495 Doi 10.1146/annurev-immunol-041015-055318
- 80 Middleton D, Curran M, Maxwell L (2002) Natural killer cells and their receptors. *Transpl Immunol* 10: 147-164 Doi 10.1016/s0966-3274(02)00062-x
- 81 Mohr A, Atif M, Balderas R, Gorochov G, Miyara M (2019) The role of FOXP3(+) regulatory T cells in human autoimmune and inflammatory diseases. *Clin Exp Immunol* 197: 24-35 Doi 10.1111/cei.13288
- 82 Nevalainen T, Autio A, Hurme M (2023) Human endogenous retroviruses of the HERV-K (HML-2) family are expressed in the brain of healthy individuals and modify the composition of the brain-infiltrating immune cells. *Heliyon* 9: e21283 Doi 10.1016/j.heliyon.2023.e21283
- 83 Nibber A, Clover L, Pettingill P, Waters P, Elger CE, Bien CG, Vincent A, Lang B (2016) Antibodies to AMPA receptors in Rasmussen's encephalitis. *Eur J Paediatr Neurol* 20: 222-227 Doi 10.1016/j.ejpn.2015.12.011

- 84 Olson HE, Lechpammer M, Prabhu SP, Ciarlini PD, Poduri A, Gooty VD, Anjum MW, Gorman MP, Loddenkemper T (2013) Clinical application and evaluation of the Bien diagnostic criteria for Rasmussen encephalitis. *Epilepsia* 54: 1753-1760 Doi 10.1111/epi.12334
- 85 Orsini A, Foadelli T, Carli N, Costagliola G, Masini B, Bonuccelli A, Savasta S, Peroni D, Consolini R, Striano P (2020) Rasmussen's encephalitis: From immune pathogenesis towards targeted-therapy. *Seizure* 81: 76-83 Doi 10.1016/j.seizure.2020.07.023
- 86 Owens GC, Chang JW, Huynh MN, Chirwa T, Vinters HV, Mathern GW (2016) Evidence for Resident Memory T Cells in Rasmussen Encephalitis. *Front Immunol* 7: 64 Doi 10.3389/fimmu.2016.00064
- 87 Owens GC, Erickson KL, Malone CC, Pan C, Huynh MN, Chang JW, Chirwa T, Vinters HV, Mathern GW, Kruse CA (2015) Evidence for the involvement of gamma delta T cells in the immune response in Rasmussen encephalitis. *J Neuroinflammation* 12: 134 Doi 10.1186/s12974-015-0352-2
- 88 Paik S, Kim JK, Shin HJ, Park EJ, Kim IS, Jo EK (2025) Updated insights into the molecular networks for NLRP3 inflammasome activation. *Cell Mol Immunol* 22: 563-596 Doi 10.1038/s41423-025-01284-9
- 89 Pardo CA, Vining EP, Guo L, Skolasky RL, Carson BS, Freeman JM (2004) The pathology of Rasmussen syndrome: stages of cortical involvement and neuropathological studies in 45 hemispherectomies. *Epilepsia* 45: 516-526 Doi 10.1111/j.0013-9580.2004.33103.x
- 90 Pasternack N, Doucet-O'Hare T, Johnson K, Consortium N, Paulsen O, Nath A (2024) Endogenous retroviruses are dysregulated in ALS. *iScience* 27: 110147 Doi 10.1016/j.isci.2024.110147

- 91 Patir A, Shih B, McColl BW, Freeman TC (2019) A core transcriptional signature of human microglia: Derivation and utility in describing region-dependent alterations associated with Alzheimer's disease. *Glia* 67: 1240-1253 Doi 10.1002/glia.23572
- 92 Peariso K, Standridge SM, Hallinan BE, Leach JL, Miles L, Mangano FT, Greiner HM (2013) Presentation, diagnosis and treatment of bilateral Rasmussen's encephalitis in a 12-year-old female. *Epileptic Disord* 15: 324-332 Doi 10.1684/epd.2013.0594
- 93 Pipi E, Nayar S, Gardner DH, Colafrancesco S, Smith C, Barone F (2018) Tertiary Lymphoid Structures: Autoimmunity Goes Local. *Front Immunol* 9: 1952 Doi 10.3389/fimmu.2018.01952
- 94 Power C, Poland SD, Blume WT, Girvin JP, Rice GP (1990) Cytomegalovirus and Rasmussen's encephalitis. *Lancet* 336: 1282-1284
- 95 Ramaswamy V, Walsh JG, Sinclair DB, Johnson E, Tang-Wai R, Wheatley BM, Branton W, Maingat F, Snyder T, Gross DW et al (2013) Inflammasome induction in Rasmussen's encephalitis: cortical and associated white matter pathogenesis. *J Neuroinflammation* 10: 152 Doi 10.1186/1742-2094-10-152
- 96 Raredon MSB, Yang J, Garritano J, Wang M, Kushnir D, Schupp JC, Adams TS, Greaney AM, Leiby KL, Kaminski Net al (2022) Computation and visualization of cell-cell signaling topologies in single-cell systems data using Connectome. *Sci Rep* 12: 4187 Doi 10.1038/s41598-022-07959-x
- 97 Rattani A, Lim J, Mistry AM, Prablek MA, Roth SG, Jordan LC, Shannon CN, Naftel RP (2019) Incidence of Epilepsy and Associated Risk Factors in Perinatal Ischemic Stroke Survivors. *Pediatr Neurol* 90: 44-55 Doi 10.1016/j.pediatrneurol.2018.08.025

- 98 Rocamonde B, Hasan U, Mathieu C, Dutartre H (2023) Viral-induced neuroinflammation: Different mechanisms converging to similar exacerbated glial responses. *Front Neurosci* 17: 1108212 Doi 10.3389/fnins.2023.1108212
- 99 Sankowski R, Bottcher C, Masuda T, Geirsdottir L, Sagar, Sindram E, Seredenina T, Muhs A, Scheiwe C, Shah MJ et al (2019) Mapping microglia states in the human brain through the integration of high-dimensional techniques. *Nat Neurosci* 22: 2098-2110 Doi 10.1038/s41593-019-0532-y
- 100 Savard M, Belanger C, Tardif M, Gourde P, Flamand L, Gosselin J (2000) Infection of primary human monocytes by Epstein-Barr virus. *J Virol* 74: 2612-2619 Doi 10.1128/jvi.74.6.2612-2619.2000
- 101 Schetters STT, Gomez-Nicola D, Garcia-Vallejo JJ, Van Kooyk Y (2017) Neuroinflammation: Microglia and T Cells Get Ready to Tango. *Front Immunol* 8: 1905 Doi 10.3389/fimmu.2017.01905
- 102 Schloder J, Shahneh F, Schneider FJ, Wieschendorf B (2022) Boosting regulatory T cell function for the treatment of autoimmune diseases - That's only half the battle! *Front Immunol* 13: 973813 Doi 10.3389/fimmu.2022.973813
- 103 Schneider-Hohendorf T, Mohan H, Bien CG, Breuer J, Becker A, Gorlich D, Kuhlmann T, Widman G, Herich S, Elpers C et al (2016) CD8(+) T-cell pathogenicity in Rasmussen encephalitis elucidated by large-scale T-cell receptor sequencing. *Nat Commun* 7: 11153 Doi 10.1038/ncomms11153
- 104 Schwab N, Bien CG, Waschbisch A, Becker A, Vince GH, Dornmair K, Wiendl H (2009) CD8+ T-cell clones dominate brain infiltrates in Rasmussen encephalitis and persist in the periphery. *Brain* 132: 1236-1246

- 105 Selck C, Dominguez-Villar M (2021) Antigen-Specific Regulatory T Cell Therapy in Autoimmune Diseases and Transplantation. *Front Immunol* 12: 661875 Doi 10.3389/fimmu.2021.661875
- 106 Shah AH, Rivas SR, Doucet-O'Hare TT, Govindarajan V, DeMarino C, Wang T, Ampie L, Zhang Y, Banasavadi-Siddegowda YK, Walbridge Set al (2023) Human endogenous retrovirus K contributes to a stem cell niche in glioblastoma. *J Clin Invest* 133: Doi 10.1172/JCI167929
- 107 Shembrey C, Foroutan M, Hollande F (2022) A new natural killer cell-specific gene signature predicting recurrence in colorectal cancer patients. *Front Immunol* 13: 1011247 Doi 10.3389/fimmu.2022.1011247
- 108 Sinclair J (2008) Human cytomegalovirus: Latency and reactivation in the myeloid lineage. *J Clin Virol* 41: 180-185 Doi 10.1016/j.jcv.2007.11.014
- 109 Smith T, Heger A, Sudbery I (2017) UMI-tools: modeling sequencing errors in Unique Molecular Identifiers to improve quantification accuracy. *Genome Res* 27: 491-499 Doi 10.1101/gr.209601.116
- 110 Sumida TS, Cheru NT, Hafler DA (2024) The regulation and differentiation of regulatory T cells and their dysfunction in autoimmune diseases. *Nat Rev Immunol* 24: 503-517 Doi 10.1038/s41577-024-00994-x
- 111 Szabo PA, Levitin HM, Miron M, Snyder ME, Senda T, Yuan J, Cheng YL, Bush EC, Dogra P, Thapa Pet al (2019) Single-cell transcriptomics of human T cells reveals tissue and activation signatures in health and disease. *Nat Commun* 10: 4706 Doi 10.1038/s41467-019-12464-3

- 112 Takahashi Y, Matsuda K, Kubota Y, Shimomura J, Yamasaki E, Kudo T, Fukushima K, Osaka H, Akasaka N, Imamura A et al (2006) Vaccination and infection as causative factors in Japanese patients with Rasmussen syndrome: molecular mimicry and HLA class I. *Clin Dev Immunol* 13: 381-387 Doi 10.1080/17402520600589522
- 113 Takahashi Y, Mogami Y, Mine J, Imai K, Koide Y, Matsuda K, Akasaka N, Konishi T, Imamura A, Inoue Y (2013) Genetic variations of immunoregulatory genes associated with Rasmussen syndrome. *Epilepsy Res* 107: 238-243 Doi 10.1016/j.epilepsyres.2013.09.004
- 114 Takei H, Wilfong A, Malphrus A, Yoshor D, Hunter JV, Armstrong DL, Bhattacharjee MB (2010) Dual pathology in Rasmussen's encephalitis: a study of seven cases and review of the literature. *Neuropathology* 30: 381-391 Doi 10.1111/j.1440-1789.2009.01079.x
- 115 Team I (2019) immunarch: An R Package for Painless Bioinformatics Analysis of T-Cell and B-Cell Immune Repertoires <http://doi.org/10.5281/zenodo.3367200>
- 116 Thilo B, Stingle R, Knudsen K, Boor R, Bien CG, Deuschl G, Lang N (2009) A case of Rasmussen encephalitis treated with rituximab. *Nat Rev Neurol* 5: 458-462 Doi 10.1038/nrneurol.2009.98
- 117 Timarova G, Lisa I, Kukumberg P (2016) Long-term effect of rituximab in a case with late-onset Rasmussen s encephalitis with anti-ganglioside IgGQ1b and anti-GAD antibodies positivity. *Case Report. Neuro Endocrinol Lett* 37: 179-183
- 118 Tingleff T, Raisanen S, Vikanes A, Sandvik L, Sugulle M, Murzakanova G, Laine K (2023) Different pathways for preterm birth between singleton and twin pregnancies: a population-based registry study of 481 176 nulliparous women. *BJOG* 130: 387-395 Doi 10.1111/1471-0528.17344

- 119 Troscher AR, Wimmer I, Quemada-Garrido L, Kock U, Gessl D, Verberk SGS, Martin B, Lassmann H, Bien CG, Bauer J (2019) Microglial nodules provide the environment for pathogenic T cells in human encephalitis. *Acta Neuropathol* 137: 619-635 Doi 10.1007/s00401-019-01958-5
- 120 Ukita M, Hamanishi J, Yoshitomi H, Yamanoi K, Takamatsu S, Ueda A, Suzuki H, Hosoe Y, Furutake Y, Taki M et al (2022) CXCL13-producing CD4⁺ T cells accumulate in the early phase of tertiary lymphoid structures in ovarian cancer. *JCI Insight* 7: Doi 10.1172/jci.insight.157215
- 121 Valkiers S, Van Houcke M, Laukens K, Meysman P (2021) ClusTCR: a Python interface for rapid clustering of large sets of CDR3 sequences with unknown antigen specificity. *Bioinformatics*: Doi 10.1093/bioinformatics/btab446
- 122 Varadkar S, Bien CG, Kruse CA, Jensen FE, Bauer J, Pardo CA, Vincent A, Mathern GW, Cross JH (2014) Rasmussen's encephalitis: clinical features, pathobiology, and treatment advances. *Lancet Neurol* 13: 195-205 Doi 10.1016/S1474-4422(13)70260-6
- 123 Venturi V, Price DA, Douek DC, Davenport MP (2008) The molecular basis for public T-cell responses? *Nat Rev Immunol* 8: 231-238 Doi 10.1038/nri2260
- 124 Vezzani A, Aronica E, Mazarati A, Pittman QJ (2013) Epilepsy and brain inflammation. *Exp Neurol* 244: 11-21 Doi 10.1016/j.expneurol.2011.09.033
- 125 Vignali DA, Collison LW, Workman CJ (2008) How regulatory T cells work. *Nat Rev Immunol* 8: 523-532 Doi 10.1038/nri2343
- 126 Villar J, Segura E (2020) Decoding the Heterogeneity of Human Dendritic Cell Subsets. *Trends Immunol* 41: 1062-1071 Doi 10.1016/j.it.2020.10.002

- 127 Vinters HV, Wang R, Wiley CA (1993) Herpesviruses in chronic encephalitis associated with intractable childhood epilepsy. *Hum Pathol* 24: 871-879
- 128 Wakim LM, Woodward-Davis A, Bevan MJ (2010) Memory T cells persisting within the brain after local infection show functional adaptations to their tissue of residence. *Proc Natl Acad Sci U S A* 107: 17872-17879 Doi 10.1073/pnas.1010201107
- 129 Wang G, Wen WX, Mead AJ, Roy A, Psaila B, Thongjuea S (2022) Processing single-cell RNA-seq datasets using SingCellaR. *STAR Protoc* 3: 101266 Doi 10.1016/j.xpro.2022.101266
- 130 Wang YS, Luo QL, Guan YG, Fan DY, Luan GM, Jing A (2021) HCMV infection and IFITM3 rs12252 are associated with Rasmussen's encephalitis disease progression. *Ann Clin Transl Neurol* 8: 558-570 Doi 10.1002/acn3.51289
- 131 Watts TH, Yeung KKM, Yu T, Lee S, Eshraghisamani R (2025) TNF/TNFR Superfamily Members in Costimulation of T Cell Responses-Revisited. *Annu Rev Immunol* 43: 113-142 Doi 10.1146/annurev-immunol-082423-040557
- 132 Wen W, Cheng J, Tang Y (2024) Brain perivascular macrophages: current understanding and future prospects. *Brain* 147: 39-55 Doi 10.1093/brain/awad304
- 133 Westfall JJ, Schwind WN, Sran S, Navarro JB, Leonard J, Pindrik JA, Pierson CR, Boue DR, Koboldt DC, Ostendorf AP et al (2022) Molecular and spatial heterogeneity of microglia in Rasmussen encephalitis. *Acta Neuropathol Commun* 10: 168 Doi 10.1186/s40478-022-01472-y
- 134 Wing K, Yamaguchi T, Sakaguchi S (2011) Cell-autonomous and -non-autonomous roles of CTLA-4 in immune regulation. *Trends Immunol* 32: 428-433 Doi 10.1016/j.it.2011.06.002

- 135 Wirenfeldt M, Clare R, Tung S, Bottini A, Mathern GW, Vinters HV (2009) Increased activation of Iba1+ microglia in pediatric epilepsy patients with Rasmussen's encephalitis compared with cortical dysplasia and tuberous sclerosis complex. *Neurobiol Dis* 34: 432-440
- 136 Woo SR, Li N, Bruno TC, Forbes K, Brown S, Workman C, Drake CG, Vignali DA (2010) Differential subcellular localization of the regulatory T-cell protein LAG-3 and the coreceptor CD4. *Eur J Immunol* 40: 1768-1777 Doi 10.1002/eji.200939874
- 137 Wu B, Zhang G, Guo Z, Wang G, Xu X, Li JL, Whitmire JK, Zheng J, Wan YY (2021) The SKI proto-oncogene restrains the resident CD103(+)CD8(+) T cell response in viral clearance. *Cell Mol Immunol* 18: 2410-2421 Doi 10.1038/s41423-020-0495-7
- 138 Xue B, Zeng T, Jia L, Yang D, Lin SL, Sechi LA, Kelvin DJ (2020) Identification of the distribution of human endogenous retroviruses K (HML-2) by PCR-based target enrichment sequencing. *Retrovirology* 17: 10 Doi 10.1186/s12977-020-00519-z
- 139 Yang R, Puranam RS, Butler LS, Qian WH, He XP, Moyer MB, Blackburn K, Andrews PI, McNamara JO (2000) Autoimmunity to munc-18 in Rasmussen's encephalitis. *Neuron* 28: 375-383
- 140 Zhang C, Sheng Q, Zhang X, Xu K, Jin X, Zhou W, Zhang M, Lv D, Yang C, Li Yet al (2023) Prioritizing exhausted T cell marker genes highlights immune subtypes in pancreatic cancer. *iScience* 26: 106484 Doi 10.1016/j.isci.2023.106484
- 141 Zhou Y, Zhou B, Pache L, Chang M, Khodabakhshi AH, Tanaseichuk O, Benner C, Chanda SK (2019) Metascape provides a biologist-oriented resource for the analysis of systems-level datasets. *Nat Commun* 10: 1523 Doi 10.1038/s41467-019-09234-6

Abbreviations

ASM, Anti-seizure medication

BCR, B cell receptor

CDR3, Complementarity determining region 3

FCD, Focal cortical dysplasia

HLA, Human Leukocyte Antigen

HHV, Human herpes virus

IgH, Immunoglobulin heavy chain

LIANA, ligand receptor analysis framework

MS, Multiple sclerosis

RE, Rasmussen encephalitis

scRNA-seq, single cell RNA sequencing

TCR, T cell receptor

UMI, Unique Molecular Identifiers

UMAP, Uniform Manifold Approximation and Projection

Declarations*Ethics approval and consent to participate*

This study was approved by the UCLA Institutional Review Board (IRB no. 18-001048). The patients or their parents or legal guardians provided informed consent for the use of the surgical remnant and blood for research purposes according to the Declaration of Helsinki. De-identified patient information including age at seizure onset, age at surgery, and gender was collected with informed consent.

Consent for publication

The patients or their parents or legal guardians provided informed consent for future publication or presentation at conferences of de-identified research results.

Availability of data and materials

NCBI Gene Expression Omnibus accession number GSE312319

Competing interests

The authors declare that they have no competing interests.

Funding

This work was funded by the RE Children's Project to GCO and in part by a DOD/CDMRP Rare Cancers Research Program Idea Award (RA220179), The Lindonlight Collective grant (GR-240004), and an NIH/NCI award (P50 CA211015) to ACW. GQ-V received support as a member of The Collaboratory at the UCLA Institute for Quantitative and Computational Biosciences.

Authors' contributions

GCO designed the study, GCO and GQ-V analyzed the data and wrote the paper, JWC processed tissue and blood specimens, AF provided the surgical specimens, HVV and SDM provided pathologically evaluated tissue sections, NS provided MRI scans, and ACW provided additional funding. All authors reviewed a draft of the manuscript.

Acknowledgements

Single cell RNA sequencing was performed by the Technology Center for Genomics and Bioinformatics, Department of Pathology and Laboratory Medicine, David Geffen School of Medicine, and multiplex immunofluorescence staining was carried out by the Translational Pathology Core Laboratory, Department of Pathology and Laboratory Medicine, David Geffen School of Medicine.

Figure Legends

Figure 1. Immune cells in sections from the three surgical specimens (Patient 738, A, B, and C; patient 754, D, E and F; patient 769, G, H and I). Scans of multiplex immunostaining for HLA-DR, CD3, CD4, CD8, and CD20 were processed in PhenoImager HT 2.0. (A, D, and G) Low power images of HLA-DR expression rendered as a histochemical stain showing focal accumulation of activated myeloid cells (scale bar = 500 microns). (B, E and H) Higher power images of CD8 T cells (red), and HLA-DR positive myeloid cells (green). C, F and I) Images of the same area showing the CD8 T cells (green), CD4 T cells (red) and B cells (tourquoise). Colored arrows point to examples of the different immune cells (scale bar = 100 microns).

Figure 2. Pie charts depict the proportion of different cell types in the three RE surgery specimens after integration of the scRNA-seq data from each library.

Figure 3. Phenotypes of the T cells and NK cells in the immune cell fractions that were isolated from the three RE surgery specimens. A) UMAP of cell clusters based on the normalized counts of the most variable genes. B) UMAPs showing the proportion of T cells and NK cells in the three surgical specimens and identification of the clusters comprising CD8 and CD4 T cells. C) Bubble plot of selected genes that distinguish between the different T cell and NK cell clusters. D) Frequency histograms showing the distribution of T cells clonotypes from the three surgical specimens among the T cell clusters. In the upper histogram the frequent clonotypes (>1%) are plotted as a percentage of the total number of frequent clonotypes from each RE case. In the lower histogram the infrequent clonotypes (<1%) are plotted in the same way. D) UMAPS showing that the most frequent clonotypes in RE cases 738 and 754 are found in several CD8 clusters whereas the most frequent clonotype in RE case 769 is almost exclusively found in a single CD4 T cell cluster (see also Table S1).

Figure 4. Pie charts depict the proportion of the frequent CD4 and CD8 T clonotypes (>1%) that are either public or private (patient-specific).

Figure 5. B cell clonotypes in RE case 738. A) Frequency distribution of the CDR3 lengths in the sample of IgH sequences from sequencing genomic DNA isolated from part of the surgical specimen. B) Chord plot showing IgH V and J gene usage. C) Proportion of clonotypes that comprise the most frequent B cell clones (>1%) resolved using ViCloD.

Figure 6. Phenotypes of the myeloid cells in the three RE surgical specimens. A) UMAP showing the clusters of myeloid cells based on the expression of the most variable genes after integration of the scRNA-seq data. B) Histogram showing the distribution of myeloid cell types among the three RE cases. C) Bubble plot of selected genes that define microglia. D) Bubble plot of genes that define monocyte-derived macrophages and dendritic cells. E) Bubble plot of genes associated with activated microglia. F) Violin plots of selected genes that distinguish between clusters of microglia.

Figure 7. Predicted ligand: receptor interactions between myeloid cells and T cells. Bubble plot showing ligand: receptor pairings that were highly ranked by seven different methods implemented in LIANA+. Consensus rank specificity and magnitude scores are between 0 (highest rank) to 1 (lowest rank) (Table S8). The bubble plot depicts 1-rank specificity and 1-rank magnitude scores. MDM, monocyte-derived macrophages, MoDC, monocyte-derived dendritic cells.

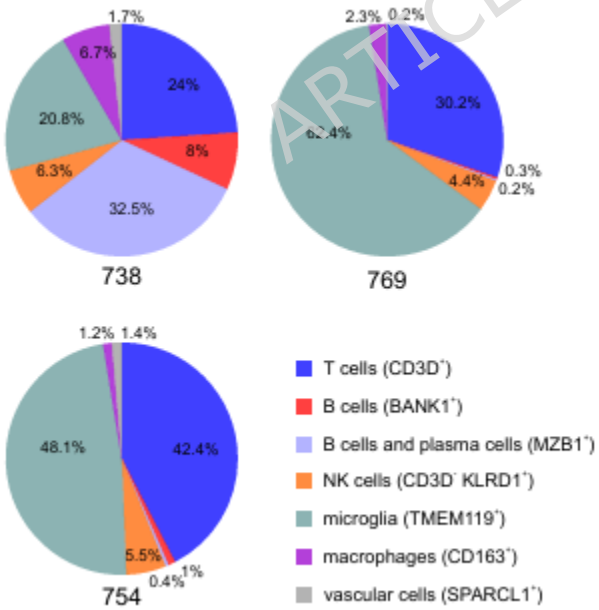
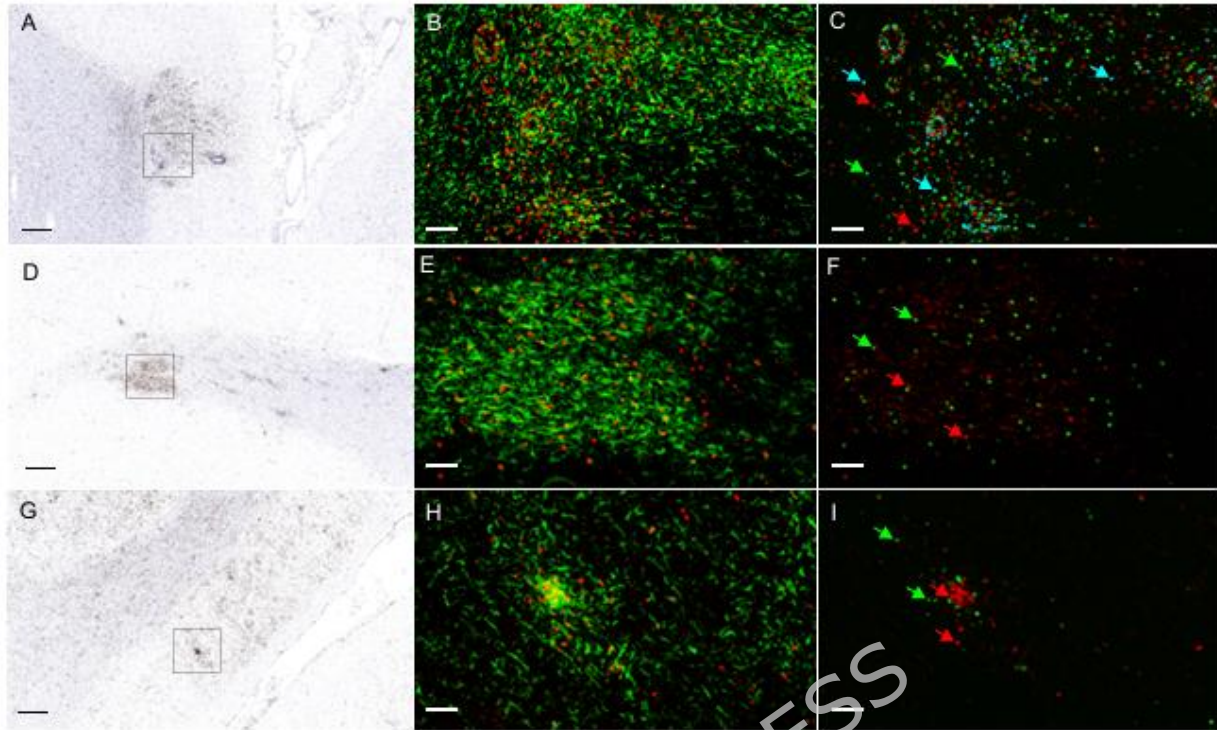
Figure 8. Locations of active HERV-K proviruses. A) HERV-K transcripts from each brain specimen were mapped to known sites of HERV-K integration and displayed in an ideogram of the human karyotype showing gene density on each chromosome. Purple pins mark the patient-specific sites, and red pins mark the sites common to the three patients. B) Venn diagrams showing the overlap between the three patients, the overlap with mapped sites of HERV-K integration from

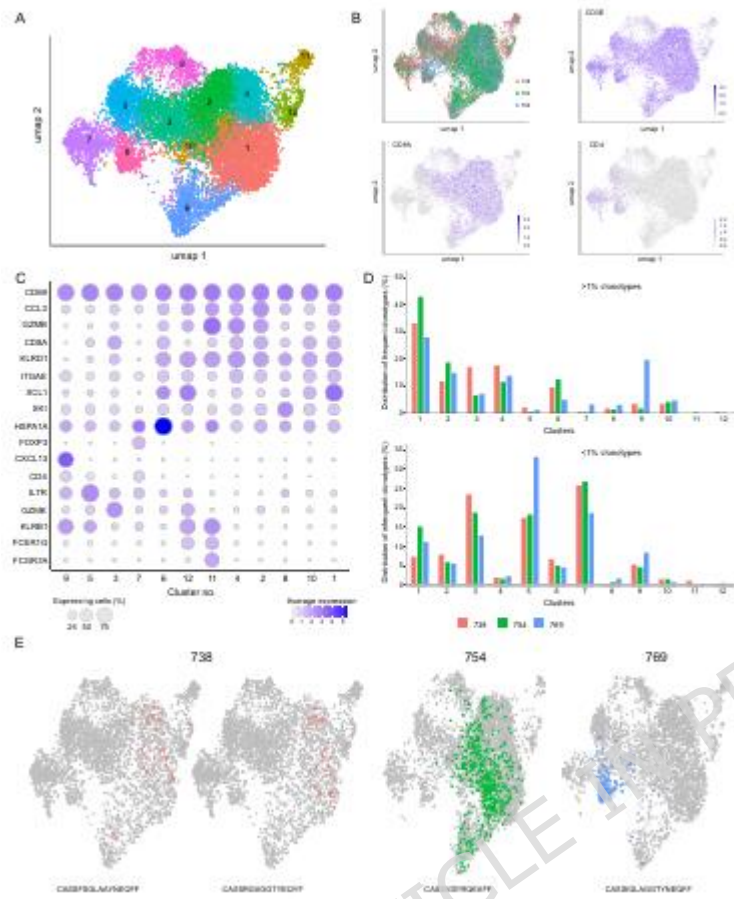
two published studies, and the overlap with active proviruses previously identified in normal brain cortex.

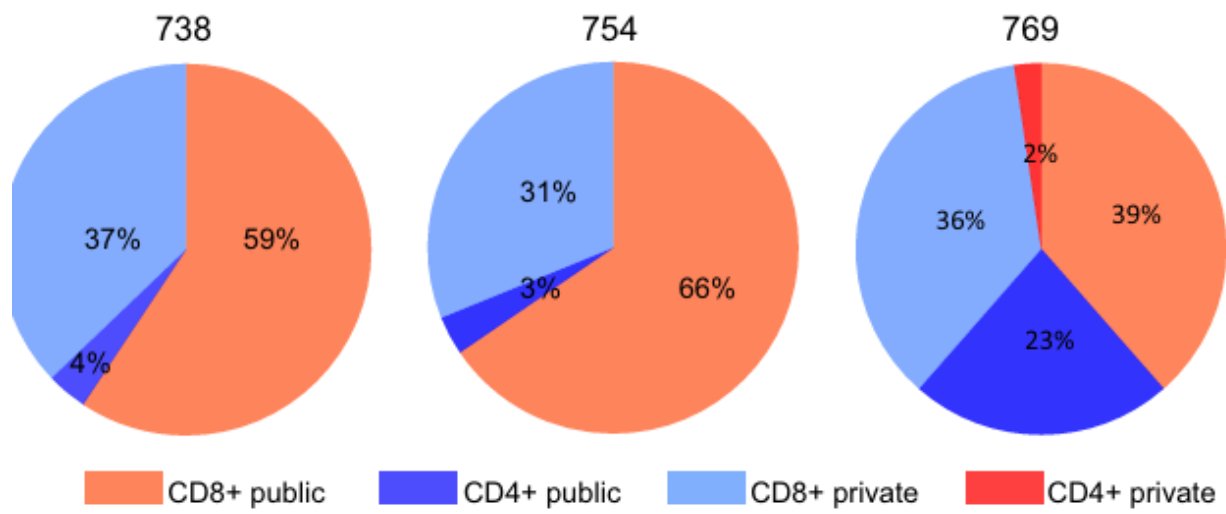
Case ID	Gender	Age at seizure onset (yr)	Age at surgery (yr)	Seizure frequency	Affected hemisphere	Anti-seizure medication	Immuno-therapy
738	male	21	26	~15 per day	right	gabapentin lamotrigine levetiracetam	IVIG 2 mo. before surgery
754	male	5	8	~1 per day	left	brivaracetam clobazam clonazepam lacosamide	none
769	female	2	5	~24 per day	right	lacosamide levetiracetam	IVIG 8 mo. before surgery

Cluster	Gene signature	Padj	NES
1	CD8 Cytokine	0.0261	1.8833
	virus responsive	0.0041	1.8937
2	T _{exhausted}	0.0021	1.8203
4	CD8 Cytokine	0.0355	1.6735
	T _{exhausted}	0.0340	1.5864
5	CD4 Naive/CM	0.0015	1.8320
	CD4/CD8	0.0034	1.7994
6	virus responsive	0.0490	1.8565
7	T _{reg}	0.0017	1.6103
11	NK	0.0002	1.6981
	CD8 Cytotoxic	0.0005	1.6877
12	NK	0.0148	1.8039

NES: normalized enrichment score







ARTICLE IN PRESS

